White Rose Research Online

eprints@whiterose.ac.uk
https://eprints.whiterose.ac.uk
Universities of Leeds, Sheffield and York

Deposited via The University of Sheffield.

White Rose Research Online URL for this paper:
https://eprints.whiterose.ac.uk/id/eprint/187872/

Version: Published Version

Article:

Bailey, N.J., Carr, M.R., David, J.P.R. et al. (2022) Growth of InAs(Bi)/GaAs quantum dots under a bismuth surfactant at high and low temperature. Journal of Nanomaterials, 2022. 5108923. ISSN: 1687-4110

https://doi.org/10.1155/2022/5108923

Reuse

This article is distributed under the terms of the Creative Commons Attribution (CC BY) licence. This licence allows you to distribute, remix, tweak, and build upon the work, even commercially, as long as you credit the authors for the original work. More information and the full terms of the licence here: https://creativecommons.org/licenses/

Takedown

If you consider content in White Rose Research Online to be in breach of UK law, please notify us by emailing eprints@whiterose.ac.uk including the URL of the record and the reason for the withdrawal request.

Hindawi
Journal of Nanomaterials
Volume 2022, Article ID 5108923, 9 pages
https://doi.org/10.1155/2022/5108923

Research Article

Growth of InAs(Bi)/GaAs Quantum Dots under a Bismuth Surfactant at High and Low Temperature

N. J. Bailey, M. R. Carr, J. P. R. David, and R. D. Richards

Electronic and Electrical Engineering Department, The University of Sheffield, S1 3JD, UK

Correspondence should be addressed to R. D. Richards; r.richards@sheffield.ac.uk

Received 10 March 2022; Accepted 18 May 2022; Published 6 June 2022

Academic Editor: Achim Trampert

Copyright © 2022 N. J. Bailey et al. This is an open access article distributed under the Creative Commons Attribution License, which permits unrestricted use, distribution, and reproduction in any medium, provided the original work is properly cited.

Indium arsenide quantum dots are of great interest for next-generation telecom optoelectronics if their emission wavelength can be red shifted into the correct range. One method to achieve this is the deposition of a surfactant, such as bismuth, during quantum dot growth. Here, we present a series of indium arsenide quantum dot layers grown using several bismuth fluxes and two different growth temperatures. The effects of bismuth flux on quantum dot morphology and optical properties are studied by atomic force microscopy and photoluminescence measurements. Bimodal distributions of quantum dots are seen at low growth temperature, while at high temperature, a single dominant distribution is seen in most of the layers. A medium bismuth flux was seen to produce the highest integrated photoluminescence intensity at high growth temperature, whereas intensity saturates between medium and high fluxes at low growth temperatures. A significant increase in uncorrected aspect ratio seen for the layer grown with a low bismuth flux at high growth temperature presents a new opportunity for control of quantum dot morphology using bismuth.

1. Introduction

Since the 1980s there has been interest in using 3-dimensional quantum confinement to alter the optical and electrical properties of semiconductors [1, 2]. One method to achieve this is to embed nanoscale semiconductor blocks within a wider band gap semiconductor. These are referred to as quantum dots (QDs). Self-assembling indium arsenide (InAs) QDs grown on gallium arsenide (GaAs) have been studied for many years [3, 4] and are of key interest due to their potential in telecoms optoelectronics both as single photon emitters and laser diodes [5, 6]. There are various challenges to using InAs QDs in these applications, but most important is red shifting the emission wavelength into the telecoms O and C bands at 1300 and 1550 nm, respectively. This has been attempted by various means, including growing larger QDs, strain/band engineering in the capping layer, or using a surfactant during QD growth. Growing thicker InAs depositions to produce larger QDs can lead to the formation of dislocated InAs islands however and negatively affect the layer properties [7, 8]. Strain engineering using metamorphic buffers has yielded promising results [9–11] and growth on indium phosphide (InP) has produced devices operating at 1550 nm [12, 13].

High QD uniformity is also desirable in these structures, particularly for laser applications in order to reduce threshold currents [5]. Surfactant deposition during QD growth has been shown to have a significant impact on the size and uniformity of InAs QDs as well as impacting QD density [14–24].

Antimony (Sb) has been studied extensively as both a capping layer material, using GaAsSb [25–27], and as a surfactant during different stages of QD growth [23, 24, 28]. By capping with GaAsSb, dramatic red shifts to QD emission have been demonstrated [25, 26]. As a pregrowth layer Sb has been shown to increase QD density [29], when used as a surfactant during QD formation, however, Sb causes a blue shift in emission. This has been shown by Lu et al. on (001) GaAs substrates and was attributed to a reduction in QD size [23]. Matsuura et al. also observed this effect and ascribed it

to an increase in the Stranski-Krastanov critical thickness [24].

Bismuth (Bi) can also be used as a surfactant during InAs QD growth. It is reported to lead to a reduction in QD density [16–18], and contrary to Sb, it has been shown to increase the average height of QDs [8, 16–18]. However, there are reports which have indicated that the effect of Bi is not straightforward. Dasika et al. [8] found that for InAs depositions of ≤2.3 monolayers (ML), Bi reduced QD density, but for depositions of ≥2.6 ML, a Bi flux increased QD density. It was also noted that Bi reduced the dislocated island density for all InAs depositions (2.3–3.3 ML), with the largest reduction for the thickest depositions. Chen et al. [19] found that a Bi flux reduced the density of QDs in the growth temperature range of 475–492°C but increased QD density for temperatures of 492–500°C. They also noted that the QDs became more uniform and the dislocated island density was reduced. Reyes et al. [17] found that low Bi fluxes < 0.03 ML/s slightly reduced photoluminescence (PL) intensity with small emission red shifts, but a flux of 0.06 ML/s caused a significant 165 meV red shift and a 68 times improvement of PL intensity.

As gallium arsenide bismide (GaAsBi) exhibits a large reduction in band gap per % Bi in GaAs [30], Bi is also a promising material for QD capping layers. Wang L et al. [20] studied the effect of Bi as a surfactant and constituent in the barrier and capping layers. They found that a 5% GaAsBi buffer reduced both the height and density of subsequent QDs when compared to GaAs. This was interpreted to indicate a delay in InAs QD nucleation caused by Bi segregation at the increased substrate temperature of 500°C for QD growth. When used in a capping layer grown at 280°C, 3% Bi induced a significant red shift of 163 meV in the emission wavelength. When the capping layer was grown at 500°C, thereby segregating all the supplied Bi; it was found to mitigate density loss during capping and improve QD uniformity.

In this work, we provide a fundamental study of the effects of Bi on InAs QDs using two layer series produced at growth temperatures of 380°C and 510°C each using several Bi fluxes. These temperatures were selected to document the effect of Bi in two regimes. The first, 380°C, is commonly used in growth of GaAsBi at which up to ~6% Bi can be incorporated [31]. The second, 510°C, is in the upper range of standard temperatures for InAs QD growth and will limit Bi to a surfactant role. Atomic force microscopy (AFM) and ensemble PL measurements are used to investigate the effects of different Bi fluxes on the morphology, density, and optical properties of the InAs QDs as well as their nucleation at low growth temperatures.

2. Methodology

The QD layers were grown in an Omicron MBE-STM system on semi-insulating (001) GaAs substrates measuring 11.8 × 11.3 mm. The substrates were initially heated to ~620°C under an arsenic (As) overpressure to desorb the native oxide. Following this, a 300 nm GaAs buffer was deposited at 580°C using an As_2:Ga atomic flux ratio of 1.7. Substrates were then cooled to the QD growth temperature of 380°C or 510°C and the As species adjusted to As_4. The change in As species was done to widen the As flux window for efficient incorporation of Bi compared to As_2, which has been discussed elsewhere [32]. Next, 2.2 ± 0.07 ML of InAs was deposited at 0.01 ML/s using an atomic flux ratio As_4:In of 30 in the presence of an additional bismuth flux. After a 10 s pause to change the As flux via a needle valve, this QD layer was buried under a 60 nm GaAs spacer grown at the same temperature as the QDs, with an atomic flux ratio As_4:Ga of 2.2. The spacer layer was added to facilitate optical measurements and prevent QD coupling [33]. Following this, an uncapped repeat QD layer was deposited to allow surface studies. The general structure of the layers is depicted in Figure 1, and the key growth conditions are included in Table 1. The GaAs growth rate was calibrated by observing RHEED oscillations and the InAs growth rate was calibrated by observing the RHEED transition at the onset of QD nucleation at 1.6 ML [34]. The As:III atomic flux ratios were calibrated using transitions between As-rich and Ga-rich reconstructions at the GaAs growth rate of 0.36 ML/s. The authors acknowledge that the conditions and structure displayed in Figure 1 do not represent the current state-of-the-art for InAs QD growth and therefore the InAs control layers grown without Bi will not display ideal characteristics. The reasoning for this basic design was to prevent ambiguity on the impact of the Bi flux on the QDs; as in the case of optimised conditions, further changes to the surface chemistry with the addition of a Bi flux would be expected to alter the previously tuned conditions and complicate any independent analysis. By instead starting with a traditional QD control layer, the full effect of the Bi flux can be observed unambiguously as has been performed on other GaAs orientations [18].

Cleaved pieces of each layer were analysed by AFM using a nominally 7 nm wide tip in 3-4 different locations with each scan covering 1 μm^2. This was to ensure a suitably large QD population was identified for each layer to perform statistical analysis on. This AFM data is presented as recorded without corrections. It is important to note that AFM is not a direct representation of the buried QDs due to compositional changes which occur during overgrowth [35, 36]. Room temperature PL measurements were taken using a liquid nitrogen cooled Ge photodetector, Horiba monochromator, and a chopped 532 nm laser operated at excitation powers of 90-900 mW. Analysis of the AFM data was performed using custom, homemade MATLAB software designed to identify individual QDs and extract their morphology characteristics. Large QDs which had minor overlap, <2 nm, due to close proximity were manually separated using this software and characterised independently. QDs with overlap larger than this which were beginning to coalesce were treated a single QD. QD populations identified from each scan were then combined into a single population for each layer. QD densities were calculated from these combined populations based on the total area covered, and height distributions were calculated as histograms indicating the probability of a QD being at a given height.

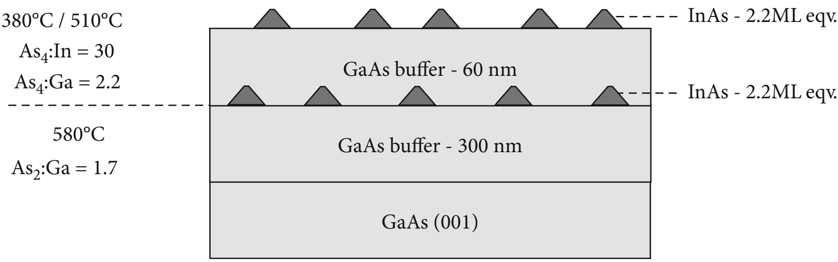

Figure 1: QD layer structure.

Table 1: Summary of growth parameters used for QD layers and ensemble properties from AFM and PL measurements. AFM statistics are split into "short" and "tall' values based on the bimodal distributions observed in Figure 2. *Values for H1 indicate QDs of low and high aspect ratio, respectively, which are discussed in Figure 3.

Layer	QD growth temperature (°C)	Bi BEP ($\times 10^{-7}$ mbar)	QD density (fit, $\times 10^{8}$ cm^{-2}) (short/tall)	Mean QD height (fit, nm) (short/tall)	PL peak (eV) (900 mW)	PL FWHM (eV) (900 mW)
L0	380	0	2.4/0	1.656/0	1.139	0.094
L1		1.2 (low)	13.4/110.2	1.367/3.329	0.992	0.051
L2		2 (med)	21.6/61.4	1.186/6.407	0.968	0.035
L3		2.7 (high)	90.0/42.4	2.009/9.712	0.968	0.033
H0	510	0	0/114.3	0/6.171	1.019	0.076
H1		1.2 (low)	31.6/81.1*	7.698/8.739*	0.987	0.043
H2		2 (med)	0/52.8	0/10	1.000	0.045
H3		2.7 (high)	0/57.6	0/12.98	0.998	0.053

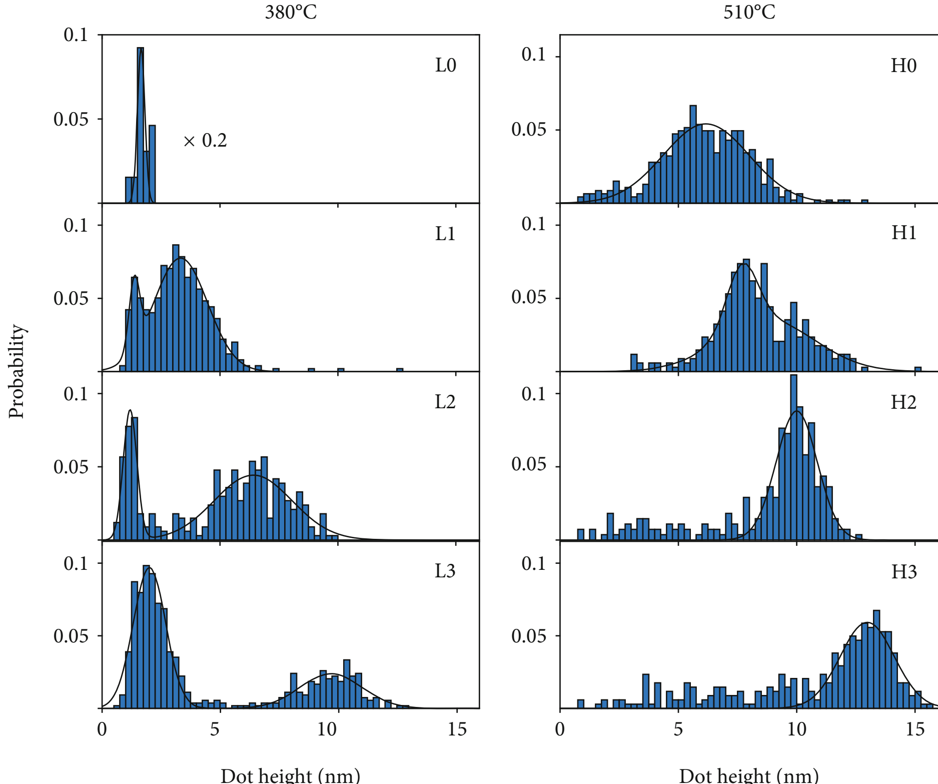

Figure 2: Histograms of QD height for all layers. Least squares Gaussian fits to each distribution are overlaid. Two Gaussians are used for layers L1 to L3 where two distributions are prominent. As H1 has also been identified to be bimodal from Figure 3, it has also been fit with two Gaussians. Peak values for the fits are noted in Table 1.

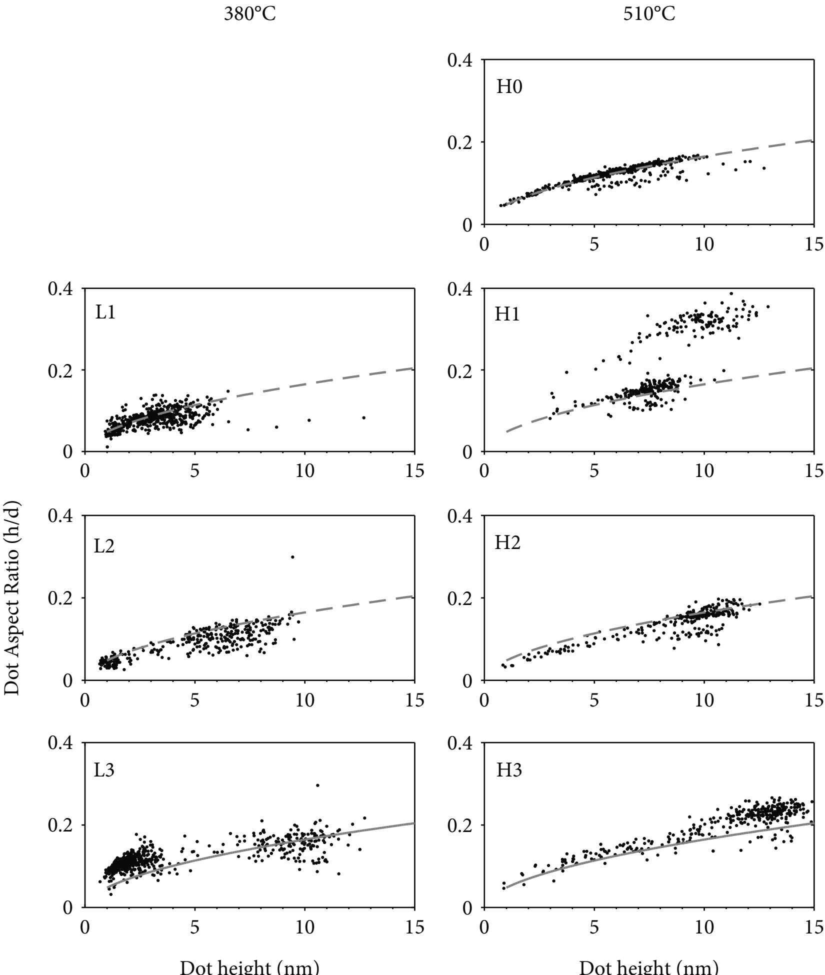

Figure 3: Plots of aspect ratio versus QD height for the layers. Layer L0 has been omitted due to the small sample size and difficulty with discerning the QDs from the wetting layer. A comparison line (dashed grey) has been added to all layers using a fit to layer H0. As the aspect ratios are calculated using uncorrected AFM data and circular approximations, they are not considered accurate; however, they are comparable across the series of layers.

3. Results and Discussion

AFM images of the layers are shown in Figure 4. It can be seen for layer L0 that at low growth temperature and without Bi, there is negligible QD formation. There appear to be some QDs starting to form, but these are at a low density and embedded in the rough wetting layer. With the addition of a Bi flux, there is a dramatic change in surface morphology where a high number of QDs form for L1. This effect is reminiscent of recent results by Lewis et al. who observed abrupt QD formation on GaAs (110) surfaces with the addition of a Bi flux [18]. With further increasing Bi flux, taller QDs are formed in layers L2 and L3. At high growth temperature, QDs are formed in all layers. The QDs grown at high temperature are also visibly more uniform compared to their low temperature counterparts.

Figure 2 displays the AFM QD height distributions for all of the samples. As seen in the raw AFM images, as the Bi flux is increased, the peak QD height increases at both growth temperatures. The layers grown at 380°C all display bimodal distributions, with a large number of short QDs between 1 and 4 nm in height, distinct from the population of taller QDs which are generally 4–13 nm tall. The exception to this is L0 which did not produce any tall QDs. The distribution of short QDs is only seen in the layers grown at 380°C and is believed to originate from 3D growth transitions below 1.6 ML which have been seen to occur at low growth temperatures [34–39]. At high growth temperature, most of the layers have single distributions and random spreads of QDs at shorter heights. H1, however, does appear display bimodal characteristics which has been observed in QD morphology comparisons and will be discussed in Figure 3. Common to all the high temperature layers are peak QD heights which are consistently higher than the low growth temperature equivalents.

Figure 5 shows the areal densities of the QDs. As the layers grown at 380°C displayed a bimodal QD height distribution, the densities of the two QD distributions have been

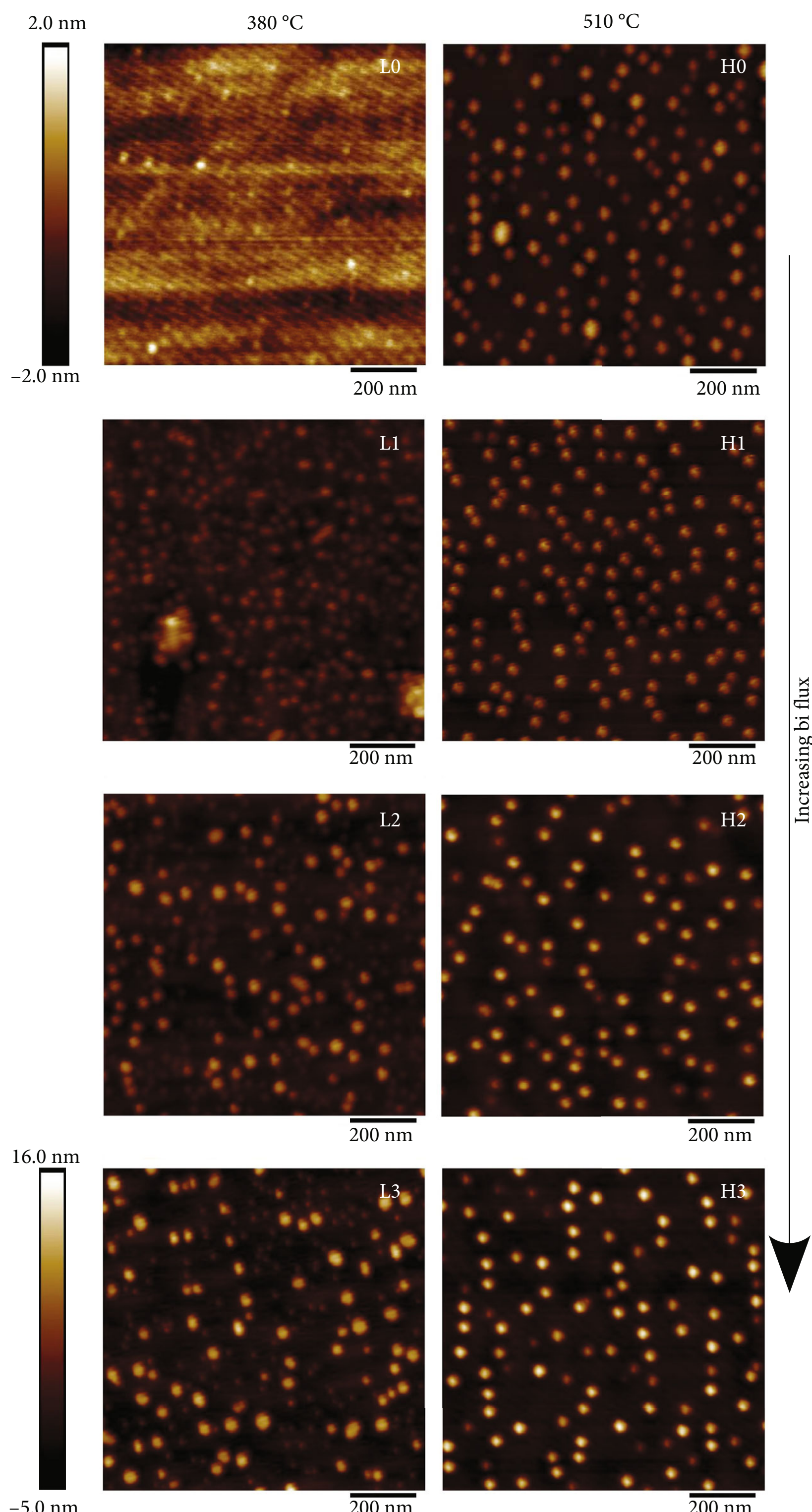

Figure 4: AFM height images of the surface QDs. Due to the low QD formation in layer L0, it has been given a smaller scale of ±2 nm. All other layers are depicted on the same scale of 16 to -5 nm.

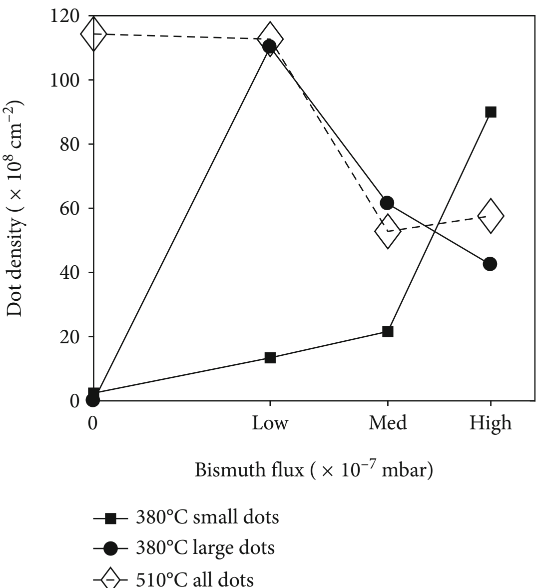

Figure 5: QD density with respect to Bi flux. Values have been calculated using the Gaussian fits to the histograms shown in Figure 2. The densities of the low and high aspect ratio dots have been combined for layer H1 in this figure.

separately recorded and were calculated using the Gaussian fits shown in Figure 2. Due to both distributions for H1 being much taller than the small dots observed in the low growth temperature layers, these have been combined in Figure 5. For layer L1, the density of tall QDs is almost identical to that of the high temperature equivalent, H1. As the Bi flux is increased at low temperature, the density of tall QDs decreases and the number of shorter QDs increases, resulting in a higher density of short QDs than tall QDs for layer L3. The impact of Bi on the QD density of the high growth temperature layers is simpler; at a low Bi flux, there is no significant change in QD density. However, as the Bi flux is increased for layers H2 and H3, there is a large decrease in QD density to 60–70% of the H1 density. This is similar to the results seen by Fan et al. [16] who noted a 50% decrease in QD density when using a Bi surfactant.

Using the area covered by each QD as identified in the MATLAB software and assuming the QDs were circular in base, an indicative aspect ratio (AR) for each QD was calculated from the uncorrected AFM data by dividing the QD height by estimated diameter. These are plotted for each layer in Figure 3 as a scatter of AR against the QD height. L0 has been omitted due to large uncertainty and the small sample size of its QD population. A dashed grey line has been added to each layer using a fit to layer H0 which had the tightest data spread and most closely represents standard InAs QD growth in this series. Looking at the low growth temperature layers, which displayed bimodal distributions in QD height, it can be seen that both height distributions follow a similar evolution in AR with height as shown by the H0 fit line. The separation of the shorter and taller QD distributions driven by increasing Bi flux can be also seen, as in Figure 2. The higher growth temperature layers generally show a tighter spread of AR compared to the low growth temperature layers, except for H1 which has two distinct distributions of QDs, which was not distinctly clear from Figure 2. Whilst these two distributions overlap in height, the taller distribution has a significantly larger aspect ratio, which is not seen in any of the other layers. The average aspect ratio for these taller QDs is approximately 0.31. A similar shift in AR to a higher value has been seen in this temperature range by Saito et al. [40]. They concluded that the driving force behind this shape transition was a combination of QD height and base strain leading to a higher aspect ratio becoming more energetically favourable. As this is only observed for the lowest Bi flux layer at this temperature and not at higher fluxes or without it, it appears that it may be possible to use Bi to control this transition.

Figure 6 shows the room temperature PL spectra taken for the layers. All of the layers display a low energy emission between 0.7 and 0.9 eV, referred to as a low energy feature (LEF); the source of this is considered to be from QD clusters and chains which have been observed by TEM elsewhere [41]. These have been seen on the surface by AFM, and due to QD dissociation during GaAs overgrowth [35, 36, 42], their densities are expected to be larger in the buried QD layers. It is noteworthy that in [41], this emission was only seen in layers grown at 300 and 450˚C and not in a layer grown at 520˚C. It is present here in all of the 510˚C layers shown in Figure 6, however, and the intensity changes little across the range of Bi fluxes, suggesting that a Bi surfactant has little effect on the formation of these clusters. As expected, due to the associated reduction of antisites and other defects, the higher growth temperature layers produced stronger QD emission in all cases. The lower growth temperature layers displayed longer wavelength emission however, with L2 and L3 having a ground state peaks at 0.968 eV. It is possible that this comparative red shift is due to a change in the QD In content between the two growth temperatures. However, as the growth rate is low, 0.01 ML/s, this is not believed to be the case as other reports have found that low growth rates reduced In-Ga intermixing [43]. Another potential cause is the incorporation of a small percentage of Bi into the QDs grown at 380˚C although it is still possible that the difference in emission wavelength is produced by morphology changes during the capping process which have been demonstrated to vary dramatically over a similar temperature range [36]. The longest wavelength achieved from the layers grown at 510˚C came from H1 with a ground state peak at 0.987 eV. This layer did not have the tallest QDs from the 510˚C series nor is it expected that the capping process would be any different for this layer compared to the others grown at this temperature. Also the solubility of Bi at this temperature prohibits incorporation. It is therefore expected that this red shift is due to emission originating from the QDs of large aspect ratio, seen in Figure 3. Whilst the statistics in Figure 3 were derived from the surface QD

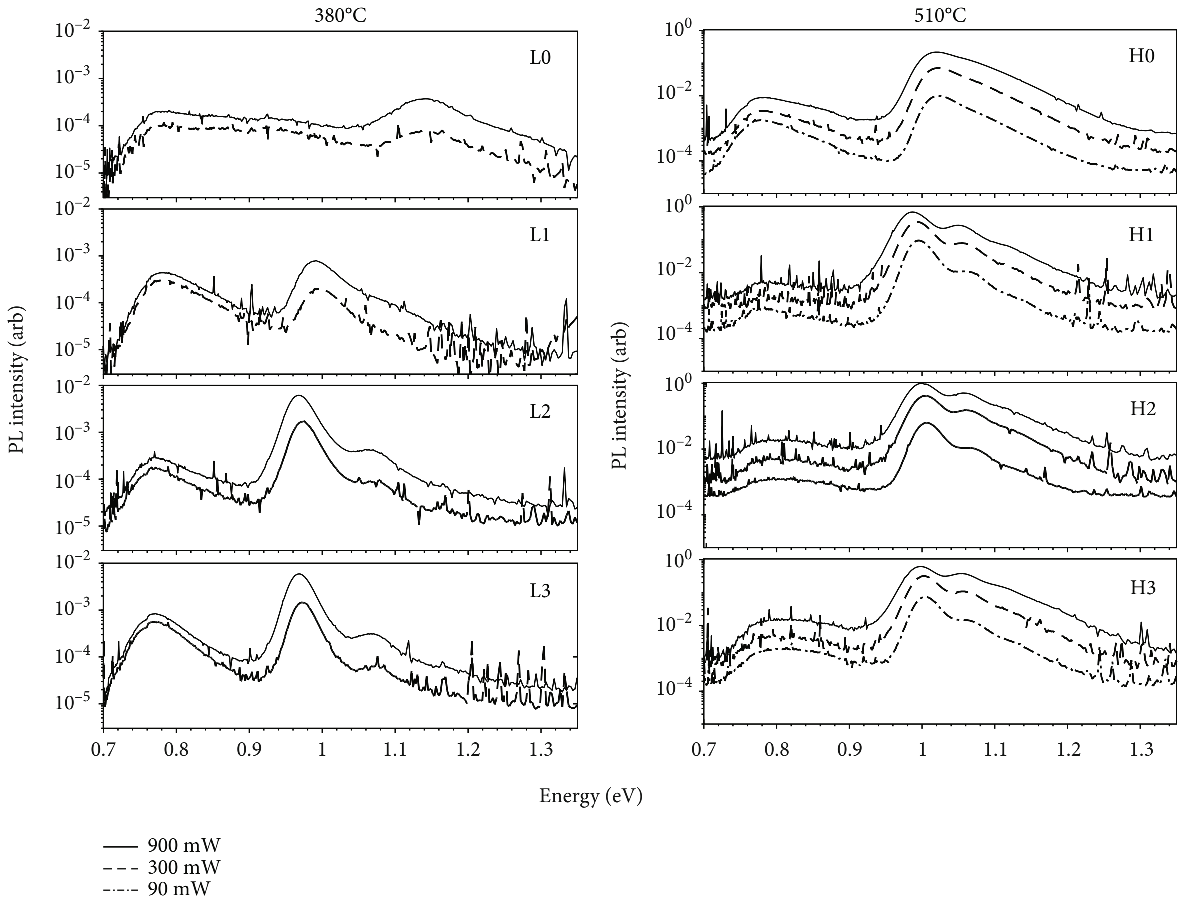

Figure 6: Room temperature photoluminescence spectra from the layers using different excitation laser powers. All spectra are normalized to the highest intensity recorded for H2. Broad luminescence (LEF) which can be seen from 0.7 to 0.9 eV is attributed to the formation of large InAs QD clusters and chains [41]. Only weak QD emission around 1.14 eV can be identified from layer L0. 90 mW data for the low growth temperature layers is omitted due to a low signal to noise ratio.

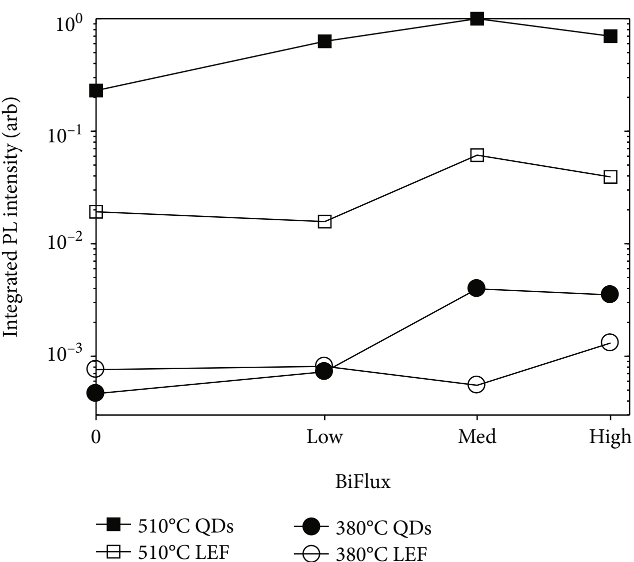

Figure 7: Integrated PL intensity from QDs (closed symbols) at 900 mW excitation plotted against bismuth flux. Values have been normalized to the maximum intensity which was recorded for layer H2. Values for the LEF in each layer have also been added (open symbols).

population, it is expected that the optically active, buried QDs will have retained a bimodal distribution despite compositional and morphology changes which occur during the capping process. The large emission red shift caused by a change in aspect ratio has been modelled by Usman et al. [44] and may be expected to be larger than the blue shift from reduced QD height. Figure 7 shows how the integrated PL (IPL) intensity of the layers varies with bismuth flux at each growth temperature. It is clear that the use of any bismuth flux produces an increase in IPL intensity at both growth temperatures. Comparing the IPL from the LEF in the layers grown at 380°C shows no clear trend; however, in the layers grown at 510°C, the IPL of the LEF increases with a decrease in dot density. The authors note that these trends in IPL intensity for both the QDs and LEF closely mimic the peak PL intensity trends for all the layers.

4. Conclusions

In summary, a systematic series of quantum dot layers grown under various bismuth fluxes and growth temperatures has been presented. Quantum dot nucleation at low growth temperatures was induced through the use of a bismuth flux as demonstrated by layers L0 and L1. In all

layers which formed quantum dots, there was a consistent increase in quantum dot height with increasing bismuth flux and a decrease in the density of large quantum dots at medium and high bismuth fluxes for both growth temperatures. Integrated photoluminescence intensity was improved compared to growth without Bi but appears to saturate between the medium and high Bi flux. The change in surface quantum dot aspect ratio observed at higher growth temperatures in layer H1 suggests that bismuth could be used to control quantum dot shape. If replicable at lower growth temperatures, where bismuth may incorporate into the dot structure, this could provide an extra pathway for MBE growth to produce quantum dots emitting at even longer wavelengths.

Data Availability

The data that support the findings of this study are available from the corresponding author upon reasonable request.

Conflicts of Interest

The authors declare no conflicts of interest in this work.

Authors' Contributions

NJB wrote the manuscript, recorded PL data, and analysed the PL and AFM data. NJB and MRC synthesised the layers. RDR and JPRD oversaw the project.

Acknowledgments

The authors would like to gratefully acknowledge Dr. Deborah Hammond and Prof. Graham Leggett from the Sheffield Surface Analysis Centre (SSAC) for the AFM measurements and Dr. Edmund Clarke for useful discussions on quantum dot growth. This work has been supported by an EPSRC grant (EP/S036792/1). The work of RDR was supported by the Royal Academy of Engineering under the Research Fellowships scheme.

References

[1] Y. Arakawa and H. Sakaki, "Multidimensional quantum well laser and temperature dependence of its threshold current," *Applied physics letters*, vol. 40, no. 11, pp. 939–941, 1982.

[2] A. I. Ekimov, A. L. Efros, and A. A. Onushchenko, "Quantum size effect in semiconductor microcrystals," *Solid State Communications*, vol. 56, no. 11, pp. 921–924, 1985.

[3] L. Goldstein, F. Glas, J. Y. Marzin, M. N. Charasse, and G. Le Roux, "Growth by molecular beam epitaxy and characterization of InAs/GaAs strained-layer superlattices," *Applied Physics Letters*, vol. 47, no. 10, pp. 1099–1101, 1985.

[4] W. J. Schaffer, M. D. Lind, S. P. Kowalczyk, and R. W. Grant, "Nucleation and strain relaxation at the InAs/GaAs(100) heterojunction," *Journal of Vacuum Science & Technology B: Microelectronics Processing and Phenomena*, vol. 1, no. 688, p. 3, 1983.

[5] M. Telford, "QD lasers go to market," *III-Vs Review*, vol. 17, no. 3, p. 28, 2004.

[6] X. Cao, M. Zopf, and F. Ding, "Telecom wavelength single photon sources," *Journal of Semiconductors*, vol. 40, no. 7, p. 071901, 2019.

[7] K. H. Schmidt, G. Medeiros-Ribeiro, J. Garcia, and P. M. Petroff, "Size quantization effects in InAs self-assembled quantum dots," *Applied Physics Letters*, vol. 70, no. 13, pp. 1727–1729, 1997.

[8] V. D. Dasika, E. M. Krivoy, H. P. Nair et al., "Increased InAs quantum dot size and density using bismuth as a surfactant," *Applied Physics Letters*, vol. 105, no. 25, p. 253104, 2014.

[9] L. Seravalli, M. Minelli, P. Frigeri, P. Allegri, V. Avanzini, and S. Franchi, "The effect of strain on tuning of light emission energy of InAs/InGaAs quantum-dot nanostructures," *Applied physics letters*, vol. 82, no. 14, pp. 2341–2343, 2003.

[10] G. Balakrishnan, S. Huang, T. J. Rotter et al., "2.0 μm wavelength InAs quantum dashes grown on a GaAs substrate using a metamorphic buffer layer," *Applied Physics Letters*, vol. 84, no. 12, pp. 2058–2060, 2004.

[11] S. Golovynskyi, L. Seravalli, O. Datsenko et al., "Comparative Study of Photoelectric Properties of Metamorphic InAs/InGaAs and InAs/GaAs Quantum Dot Structures," *Nanoscale research letters*, vol. 12, no. 1, 2017.

[12] S. Anantathanasarn, Y. Barbarin, N. I. Cade et al., "Wavelength tunable InAs/InP(100) quantum dots in 1.55-μm telecom devices," *Materials Science and Engineering: B*, vol. 147, no. 2-3, pp. 124–130, 2008.

[13] S. G. Li, Q. Gong, C. F. Cao et al., "The developments of InP-based quantum dot lasers," *Infrared Physics & Technology*, vol. 60, no. 216, p. 224, 2013.

[14] B. N. Zvonkov, I. A. Karpovich, N. V. Baidus, D. O. Filatov, S. V. Morozov, and Y. Y. Gushina, "Surfactant effect of bismuth in the MOVPE growth of the InAs quantum dots on GaAs," *Nanotechnology*, vol. 11, no. 4, pp. 221–226, 2000.

[15] H. Okamoto, T. Tawara, H. Gotoh, H. Kamada, and T. Sogawa, "Growth and characterization of telecommunication-wavelength quantum dots using Bi as a surfactant," *Japanese Journal of Applied Physics*, vol. 49, no. 6, p. 06GJ01, 2010.

[16] D. Fan, Z. Zeng, V. G. Dorogan et al., "Bismuth surfactant mediated growth of InAs quantum dots by molecular beam epitaxy," *Journal of Materials Science: Materials in Electronics*, vol. 24, no. 5, pp. 1635–1639, 2013.

[17] D. F. Reyes, D. Gonzalez, F. Bastiman et al., "Photoluminescence Enhancement of InAs(Bi) Quantum Dots by Bi Clustering," *Applied Physics Express*, vol. 6, no. 4, p. 042103, 2013.

[18] R. B. Lewis, A. Trampert, E. Luna, J. Herranz, C. Pfüller, and L. Geelhaar, "Bismuth-surfactant-induced growth and structure of InAs/GaAs(110) quantum dots," *Semiconductor Science and Technology*, vol. 34, no. 10, p. 105016, 2019.

[19] X. Y. Chen, Y. Gu, Y. J. Ma et al., "Growth mechanisms for InAs/GaAs QDs with and without Bi surfactants," *Materials Research Express*, vol. 6, no. 1, p. 015046, 2019.

[20] L. Wang, W. Pan, X. Chen, X. Wu, J. Shao, and S. Wang, "Influence of Bi on morphology and optical properties of InAs QDs," *Optical Materials Express*, vol. 7, no. 12, p. 4249, 2017.

[21] D. Guimard, M. Nishioka, S. Tsukamoto, and Y. Arakawa, "Effect of antimony on the density of InAs/Sb:GaAs(100) quantum dots grown by metalorganic chemical-vapor deposition," *Journal of Crystal Growth*, vol. 298, no. 548, p. 552, 2007.

[22] N. Kakuda, T. Yoshida, and K. Yamaguchi, "Sb-mediated growth of high-density InAs quantum dots and GaAsSb

embedding growth by MBE," *Applied surface science*, vol. 254, no. 24, pp. 8050–8053, 2008.

[23] X. Lu, N. Kumagai, Y. Minami, T. Kitada, and T. Isu, "Effects of Sb-soak on InAs quantum dots grown on (001) and (113)B GaAs substrates," *Journal of Crystal Growth*, vol. 477, no. 221, p. 224, 2017.

[24] T. Matsuura, T. Miyamoto, T. Kageyama et al., "Scanning Force Microscopic Studies ofEscherichia coliRibosomes on Solid Substrate Surface," *Japanese journal of applied physics*, vol. 43, no. 7B, pp. 4599–4601, 2004.

[25] A. Salhi, S. Alshaibani, Y. Alaskar, A. Albadri, A. Alyamani, and M. Missous, "Tuning the optical properties of InAs QDs by means of digitally-alloyed GaAsSb strain reducing layers," *Applied Physics Letters*, vol. 113, no. 10, p. 103101, 2018.

[26] Z. Zhang, Y. Huang, P. J. Reece, and S. P. Bremner, "Influence of GaAsSb structural properties on the optical properties of InAs/GaAsSb quantum dots," *Physica E: Low-dimensional Systems and Nanostructures*, vol. 94, no. 7, p. 14, 2017.

[27] Y. A. Liao, W. T. Hsu, S. H. Huang, P. C. Chiu, J. I. Chyi, and W. H. Chang, "Band alignment tuning of InAs quantum dots with a thin AlGaAsSb capping layer," *Applied Physics Letters*, vol. 102, no. 17, p. 173104, 2013.

[28] L. Dai, S. P. Bremner, S. Tan, S. Wang, G. Zhang, and Z. Liu, ""Raman scattering study on Sb spray InAs/GaAs quantum dot nanostructure systems," *Nanoscale research letters*, vol. 10, no. 1, pp. 1–6, 2015.

[29] K. Yamaguchi and T. Kanto, "Self-assembled InAs quantum dots on GaSb/GaAs(0 0 1) layers by molecular beam epitaxy," *Journal of Crystal Growth*, vol. 275, no. 1-2, pp. e2269–e2273, 2005.

[30] S. Francoeur, M. J. Seong, A. Mascarenhas, S. Tixier, M. Adamcyk, and T. Tiedje, "Band gap of GaAs1−xBix, 0<x<3.6%," *Applied physics letters*, vol. 82, no. 22, pp. 3874–3876, 2003.

[31] R. D. Richards, N. J. Bailey, Y. Liu, T. B. Rockett, and A. R. Mohmad, "GaAsBi: From Molecular Beam Epitaxy Growth to Devices," *Physica Status Solidi (b)*, vol. 259, no. 2, p. 2100330, 2022.

[32] R. D. Richards, F. Bastiman, C. J. Hunter et al., "Molecular beam epitaxy growth of GaAsBi using As2 and As4," *Journal of Crystal Growth*, vol. 390, no. 120, p. 124, 2014.

[33] X. D. Wang, N. Liu, C. K. Shih, S. Govindaraju, and A. L. Holmes Jr., "Spatial correlation-anticorrelation in strain-driven self-assembled InGaAs quantum dots," *Applied Physics Letters*, vol. 85, no. 8, pp. 1356–1358, 2004.

[34] F. Patella, F. Arciprete, M. Fanfoni, A. Balzarotti, and E. Placidi, "Apparent critical thickness versus temperature for InAs quantum dot growth on GaAs(001)," *Applied physics letters*, vol. 88, no. 16, p. 161903, 2006.

[35] H. Eisele, A. Lenz, R. Heitz et al., "Change of InAs/GaAs quantum dot shape and composition during capping," *Journal of Applied Physics*, vol. 104, no. 12, p. 124301, 2008.

[36] Q. Gong, P. Offermans, R. Noetzel, P. M. Koenrad, and J. H. Wolter, "Capping process of InAs/GaAs quantum dots studied by cross-sectional scanning tunneling microscopy," *Applied physics letters*, vol. 85, no. 23, pp. 5697–5699, 2004.

[37] H. Kissel, U. Müller, C. Walther et al., "Size distribution in self-assembled InAs quantum dots on GaAs (001) for intermediate InAs coverage," *Physical Review B*, vol. 62, no. 11, pp. 7213–7218, 2000.

[38] A. Polimeni, A. Patane, M. Capizzi, F. Martelli, L. Nasi, and G. Salviati, "Self-aggregation of quantum dots for very thin InAs layers grown on GaAs," *Physical Review B*, vol. 53, no. 8, pp. R4213–R4216, 1996.

[39] A. Patane, M. Grassi Alessi, F. Intonti et al., "Self-aggregated InAs quantum dots in GaAs," *Journal of applied physics*, vol. 83, no. 10, pp. 5529–5535, 1998.

[40] H. Saito, K. Nishi, and S. Sugou, "Shape transition of InAs quantum dots by growth at high temperature," *Applied Physics Letters*, vol. 74, no. 9, pp. 1224–1226, 1999.

[41] V. M. Ustinov, A. E. Zhukov, A. R. Kovsh et al., "Long-wavelength emission from self-organized InAs quantum dots on GaAs substrates," *Microelectronics journal*, vol. 31, no. 1, pp. 1–7, 2000.

[42] R. Songmuang, S. Kiravittaya, and O. G. Schmidt, "Shape evolution of InAs quantum dots during overgrowth," *Journal of Crystal Growth*, vol. 249, no. 3-4, pp. 416–421, 2003.

[43] P. B. Joyce, T. J. Krzyzewski, G. R. Bell et al., "Effect of growth rate on the size, composition, and optical properties of InAs/GaAs quantum dots grown by molecular-beam epitaxy," *Physical Review B*, vol. 62, no. 16, pp. 10891–10895, 2000.

[44] M. Usman, H. Ryu, I. Woo, D. S. Ebert, and G. Klimeck, "Moving Toward Nano-TCAD Through Multimillion-Atom Quantum-Dot Simulations Matching Experimental Data," *IEEE Transactions on Nanotechnology*, vol. 8, no. 3, pp. 330–344, 2009.